

Performance and stability-enhanced inorganic perovskite light-emitting devices by employing triton X-100

Ao Chen(陈翱), Peng Wang(王鹏), Tao Lin(林涛), Ran Liu(刘然), Bo Liu(刘波), Quan-Jun Li(李全军), and Bing-Bing Liu(刘冰冰)

Citation: Chin. Phys. B, 2021, 30 (**4**): 048506. DOI: 10.1088/1674-1056/abcf47
Journal homepage: http://cpb.iphy.ac.cn; http://iopscience.iop.org/cpb

What follows is a list of articles you may be interested in

PBTI stress-induced *1/f* noise in n-channel FinFET

Dan-Yang Chen(陈丹旸), Jin-Shun Bi(毕津顺), Kai Xi(习凯), and Gang Wang(王刚)
Chin. Phys. B, 2020, 29 (**12**): 128501. DOI: 10.1088/1674-1056/abaee4

In-memory computing to break the memory wall

Xiaohe Huang(黄晓合), Chunsen Liu(刘春森), Yu-Gang Jiang(姜育刚), Peng Zhou(周鹏)
Chin. Phys. B, 2020, 29 (**7**): 078504. DOI: 10.1088/1674-1056/ab90e7

Multistability and coexisting transient chaos in a simple memcapacitive system

Fu-Ping Wang(王富平), Fa-Qiang Wang(王发强)
Chin. Phys. B, 2020, 29 (**5**): 058502. DOI: 10.1088/1674-1056/ab7e98

Flexible white top-emitting organic light-emitting diode with a MoO_x roughness improvement layer

Chen Shu-Fen, Guo Xu, Wu Qiang, Zhao Xiao-Fei, Shao Ming, Huang Wei
Chin. Phys. B, 2013, 22 (**12**): 128506. DOI: 10.1088/1674-1056/22/12/128506

Improvement in electroluminescence performance of n-ZnO/Ga_2O_3/p-GaN heterojunction light-emitting diodes

Zhang Li-Chun, Zhao Feng-Zhou, Wang Fei-Fei, Li Qing-Shan
Chin. Phys. B, 2013, 22 (**12**): 128502. DOI: 10.1088/1674-1056/22/12/128502

Performance and stability-enhanced inorganic perovskite light-emitting devices by employing triton X-100*

Ao Chen(陈翱)[1,2], Peng Wang(王鹏)[1], Tao Lin(林涛)[1], Ran Liu(刘然)[1], Bo Liu(刘波)[1,†], Quan-Jun Li(李全军)[1,‡], and Bing-Bing Liu(刘冰冰)[1]

[1] *State Key Laboratory of Superhard Materials, Jilin University, Changchun* 130012, *China*
[2] *Changchun Institute of Optics, Fine Mechanics and Physics, Chinese Academy of Sciences, Changchun* 130033, *China*

(Received 3 September 2020; revised manuscript received 4 October 2020; accepted manuscript online 1 December 2020)

Significantly enhanced electroluminescence performance and stability of all-inorganic perovskite light-emitting devices (PeLEDs) have been achieved by adding triton X-100 into the perovskite precursors. The small perovskite grains arranged tightly and formed large grains as the triton X-100 were introduced. Thus the nonradiative defects originated from Pb atoms at the grain boundaries were highly passivated by triton X-100 and resulted in the promotion of PeLED performance, including a turn-on voltage of 3.2 V, a brightness of 63500 cd/m^2, a current efficiency of 17.4 cd/A, and a prolonged lifetime of 2 h in air.

Keywords: electroluminescence performance, stability, perovskite light-emitting devices (PeLEDs), triton X-100

PACS: 85.60.–q, 85.60.Bt, 85.60.Jb **DOI:** 10.1088/1674-1056/abcf47

1. Introduction

Nowadays, perovskite light-emitting devices (PeLEDs) have attracted widely scientific interest due to the outstanding optical and electrical characteristics of metal halide perovskites, such as high photoluminescence quantum efficiency (PLQY), high color purity, long diffusion length, and high charge-carrier mobility, *etc*.[1–6] During the past five years, the lead halide perovskite-based PeLED has been greatly boosted, the maximum current efficiency (CE) of the devices has been promoted from 0.3 cd/A to 42.9 cd/A.[7,8] And the record of the maximum external quantum efficiency (EQE) of green and red emitted devices are all over 20%.[5,6,9,10] Among all these reported PeLEDs, the ones based on the all-inorganic perovskite of cesium lead bromide ($CsPbBr_3$), show excellent thermal and chemical stability, together with high quantum yield.[11–15] However, the defects, among the grain interfaces formed during perovskite crystal growing, hindered the improvement of the device performance.[3,4,16,17] To reduce nonradiative recombination and achieve high efficiency all-inorganic PeLEDs, one of the positive strategies is to employ additives into the perovskite precursors. Surfactants, such as polyethylene glycol,[18] tween 20,[19] poly(2-ethyl-2-oxazoline),[20] and tetrabutylammonium bromide,[13] have been reported to passivate defects and suppress nonradiative recombination at grain boundaries. Therefore, the proper selection of additives for defect passivation in perovskite films is of an important way to improve the PeLED performance.

In this work, a nonionic surfactant triton X-100 was employed into the all-inorganic perovskite $CsPbBr_3$ precursors to passivate defects at the grain boundaries. In contrast with the control perovskite film, perovskite film with triton X-100 shows tightly arranged grains, and reduced grain boundaries. Thus the nonradiative defects at the grain boundaries were highly suppressed and enhanced PeLED performance and stability were achieved, including a turn-on voltage of 3.2 V, a brightness of 63500 cd/m^2, a current efficiency of 17.4 cd/A, and a prolonged lifetime of 2 h in air. Our results would provide an efficient approach in obtaining the well-performed all-inorganic PeLEDs.

2. Experiment procedure

Figures 1(a) and 1(b) show the PeLED structure and the molecule structure of the additive triton X-100, respectively. The device with a popular structure as shown in Fig. 1(a). Before the device fabrication, the perovskite precursor solution with a concentration of 145 mg/mL was prepared, in which CsBr and $PbBr_2$ were dissolved in anhydrous DMSO. Then 25-mg/mL triton X-100 in DMSO was added into the perovskite precursors with different volume ratios. PeLEDs were constructed on cleaned and oxygen plasma treated ITO electrodes. Then filtered poly (ethylenedioxythiophene):polystyrenesulfonate (PEDOT:PSS) was spin-coated

*Project supported by the National Key Research and Development Program of China (Grant Nos. 2018YFA0305900 and 2016YFA0300404), the National Natural Science Foundation of China (Grant Nos. 11874172, 11374120, 11634004, and 51320105007), and the Science and Technology Innovative Research Project of Jilin University, China (Grant No. 2017TD-01).

†Corresponding author. E-mail: jluliubo@jlu.edu.cn
‡Corresponding author. E-mail: liquanjun@jlu.edu.cn

© 2021 Chinese Physical Society and IOP Publishing Ltd

on the ITO electrodes then baked to form a 30-nm thick film. Afterwards, transfer the substrates into a glovebox for the perovskite film deposition to form a 50-nm thick perovskite emitting layer. Finally, 30-nm TPBi, 1-nm LiF, and 100-nm Al were deposited successively in a thermal evaporation chamber at a pressure below 5.0×10^{-5} Pa. The effective area of devices was 0.01 cm^2.

After device fabrication, several measurements were carried out. Scanning electron microscope (SEM) images were measured by a Hitachi S4800 microscope. Current density–voltage–luminance characteristics of PeLEDs were measured using a Keithley 2400 source meter and a luminance meter (LS-110, Konica Minolta). Electroluminescence (EL) spectra were tested by an Avantes Avaspec 2048 spectrometer. All these measurements were performed in air.

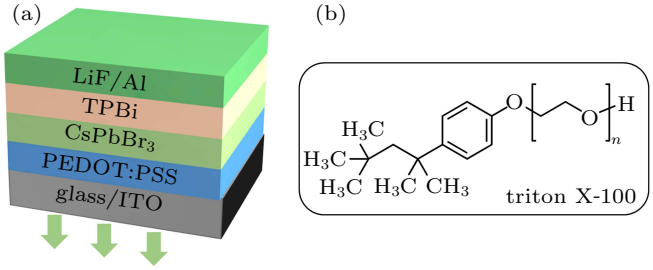


Fig. 1. (a) Schematic representation of $CsPbBr_3$ PeLED. (b) Molecule structure of triton X-100.

3. Results and discussion

To study the affection of triton X-100 on the EL performance of PeLEDs, a series of devices with different triton X-100:$CsPbBr_3$ volume ratios as the emission layers have been fabricated. Figure 2 shows the current density–voltage (J–V), luminance–voltage (L–V), CE–voltage (CE–V), as well as EQE–voltage (EQE–V) curves for these PeLEDs, and the detailed device parameters are summarized in Table 1.

Table 1. Device parameters of PeLEDs.

Triton X-100 (%)	V_{on} (V)	L_{max} (cd/m^2)	CE_{max} (cd/A)	EQE_{max} (%)
0	3.2	8990	2.14	0.12
10	3.2	42300	13.7	0.80
20	3.2	63500	17.4	1.03
30	3.2	56500	15.8	0.92

For the PeLED without triton X-100, it shows poor EL characteristics with a turn-on voltage (V_{on}) of 3.2 V, a maximum luminance (L_{max}) of 8990 cd/m^2, a maximum CE (CE_{max}) of 2.14 cd/A, and a maximum EQE (EQE_{max}) of 0.12%, respectively. As a 10% ratio of triton X-100 was added into the perovskite precursor solution, the L_{max}, CE_{max}, and EQE_{max} of the PeLEDs were promoted significantly, which values are 42300 cd/m^2, 13.7 cd/A, and 0.80%, respectively. When the ratio of triton X-100 was increased to 20%, the PeLED displays an optimized performance, including an L_{max} of 63500 cd/m^2, a CE_{max} of 17.4 cd/A, and an EQE_{max} of 1.03%. But as the triton X-100 ratio further increased to 30%, the device performance decreases again. The similar device structures of PeLEDs with different triton X-100:$CsPbBr_3$ volume ratios result in similar electrical performance, which was found expression in the similar J–V curves.

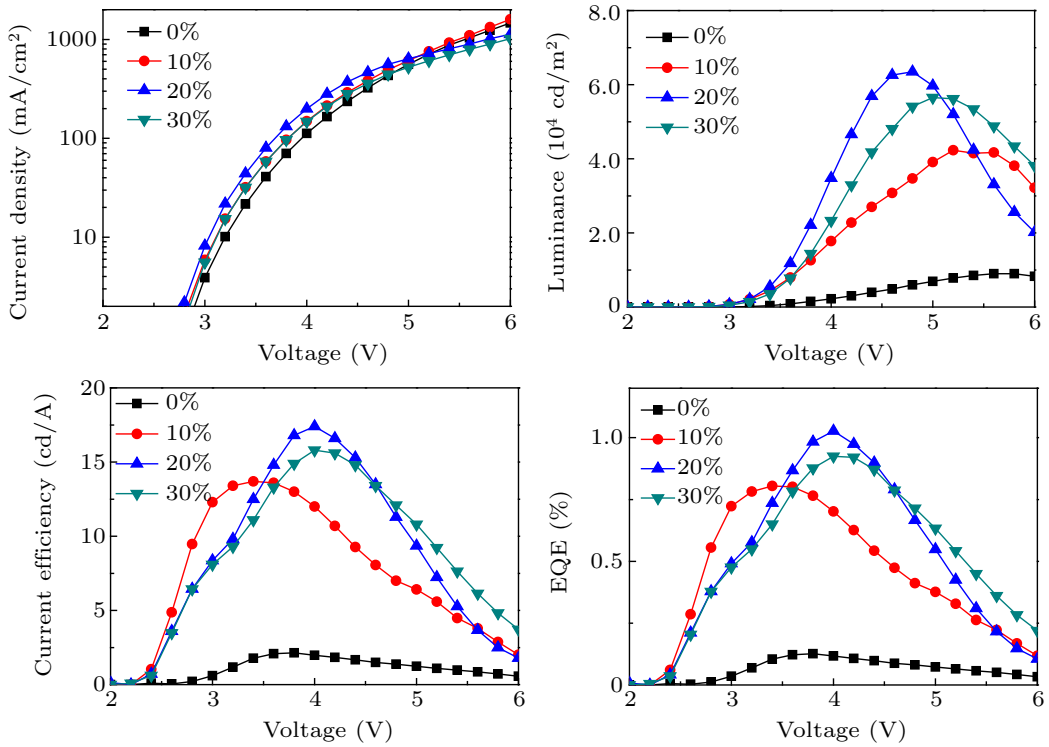


Fig. 2. (a) J–V, (b) L–V, (c) CE–V, (d) EQE–V curves for the PeLEDs with different volume ratios (triton X-100:$CsPbBr_3$).

In order to explore the affection of triton X-100 on the morphology of $CsPbBr_3$ films, SEM images of $CsPbBr_3$ films with various volume ratios of triton X-100 have been measured, which are shown in Fig. 3. For the pure $CsPbBr_3$ film (0%, Fig. 3(a)), it is mainly composed by small grains with the crystal size of about 100 nm. As a small amount of triton X-100 (10% in volume ratio) was introduced into the $CsPbBr_3$ films, the small perovskite grains arranged one by one and became irregular large grains over hundreds nanometers (Fig. 3(b)). As the triton X-100 ratio increased to 20%, the grains further enlarged to over 500 nm, which is seen clearly from Fig. 3(c). As a result, the tightly arranged grains rendered the grain boundaries in the perovskite film sharply reduced, which would decrease the defects between grain boundaries distinctly.[21–23] But when the triton X-100 ratio further increased to 30%, the grain size stopped growing and became small and separated, then grain boundaries and defects at these boundaries would increase again, and thus decrease the device performance. The grain boundaries changes is consistent with the promoted EL performance as shown in Fig. 2. The device EL performance increases as the grain boundaries decreasing and decreases as the grain boundaries increasing. In a word, the triton X-100's introduction results in the defects passivated at the grain boundaries and finally enhanced EL performance.[24–26]

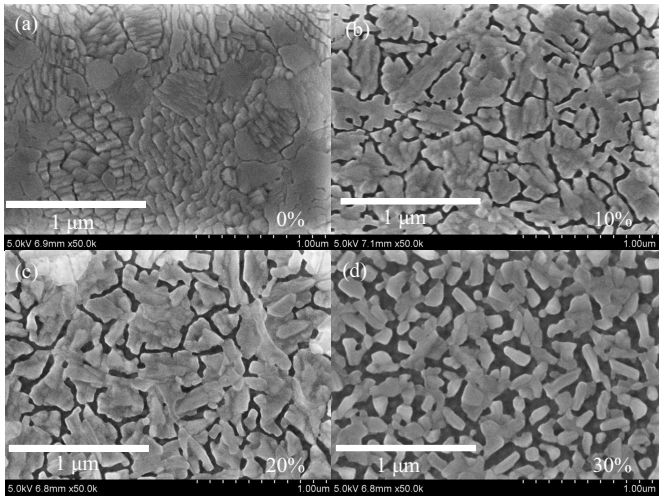


Fig. 3. SEM images of perovskite films with various volume ratios (triton X-100:$CsPbBr_3$) (a) 0%, (b) 10%, (c) 20%, and (d) 30%.

To further investigate the affection of triton X-100 on the free carriers and exciton kinetics, the time-resolved PL decay measurement was carried out and shown in Fig. 4. After the introduction of triton X-100, the PL intensity is significantly enhanced and PLQYs of the perovskite films with and without 20% triton X-100 are 8.77, and 1.93%, respectively. The PL lifetime of the perovskite film with 20% triton X-100 is also dramatically prolonged with an average time of 14.31 ns which is 8 times higher than that of the neat $CsPbBr_3$ films (1.75 ns) fitted by tri-exponential curves. This indicates the defects are suppressed at the grain boundaries, thus enhancing the PL performance. The nonradiative decay rate also can be deduced from the following equation:

$$\mathrm{PLQY} = \frac{k_\mathrm{r}}{k_\mathrm{r} + k_\mathrm{nr}},$$

$$\tau_\mathrm{avg} = \frac{1}{k_\mathrm{r} + k_\mathrm{nr}},$$

where k_r and k_nr are the radiative and nonradiative decay rates, respectively. The nonradiative decay rate k_nr can be expressed as:

$$k_\mathrm{nr} = \frac{1 - \mathrm{PLQY}}{\tau_\mathrm{avg}}.$$

Therefore, the nonradiative decay rate of the perovskite film with 20% triton X-100 can be calculated, and the value is 6.4×10^7 s^{-1}, which is lower than that of the control film (5.6×10^8 s^{-1}). The decreased nonradiative decay rate of the triton X-100 doped perovskite film indicates the reduced defects and ion migration at the grain boundaries.

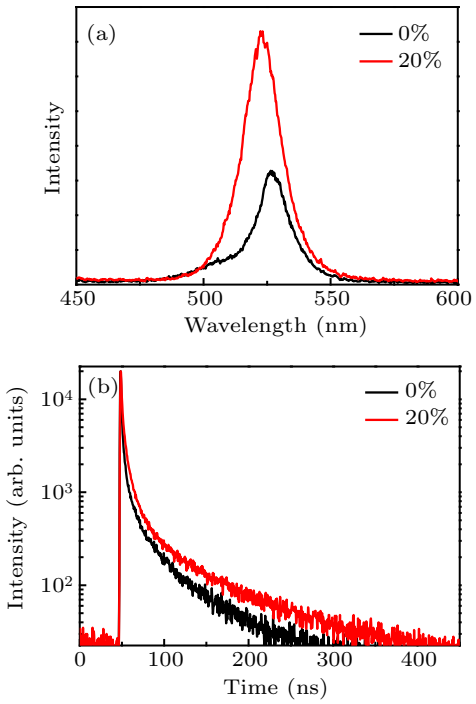


Fig. 4. (a) PL and (b) TRPL spectra of perovskite films with and without 20% triton X-100.

The stabilities of the EL devices have also been studies, figure 5 shows the EL spectra and the lifetime of the PeLED with 20% triton X-100. The EL spectra of the PeLED with 20% triton X-100 displays a stable green emitting spectrum with a peak centered at 521 nm. And the intensity of the light emission increases as the increased bias from 4 V to 6 V, and then decreases at 7 V. There is seen no obvious peak drift in Fig. 5(a), indicating the emission stability of the PeLED with 20% triton X-100. The time-dependent EL stabilities of the devices with and without 20% triton X-100 have been measured under a constant applied current without encapsulation and shown in Fig. 5(b). PeLED without triton X-100 shows a

severe degradation, it took only 36 min for the lifespan to decline by half, while the value for the PeLED with 20% triton X-100 was about 2 h. Compared with the controlled PeLED, the significantly prolonged lifetime for the triton X-100 based device can be contributed to the passivated boundaries and reduced defect state densities by employed triton X-100.

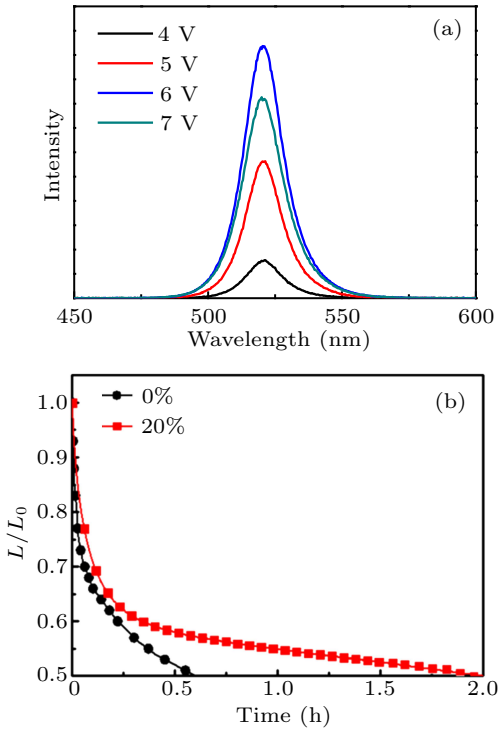


Fig. 5. (a) EL spectra of PeLEDs with 20% triton X-100 under different voltages. (b) Lifetime curves of PeLEDs with and without 20% triton X-100.

4. Conclusion

In summary, enhanced EL performance and stability of all-inorganic PeLEDs have been obtained by using a nonionic surfactant triton X-100. This surfactant promoted the formation of tightly arranged grains in the $CsPbBr_3$ films, reducing the grain boundaries in the perovskite film significantly, and resulting in decreased nonradiative decay between grain boundaries. As a result, the EL parameters were effectively enhanced with a maximum brightness of 63500 cd/m^2, a maximum current efficiency of 17.4 cd/A and a prolonged lifetime of 2 h. This work will help us to investigate the affection of the nonionic surfactant on the $CsPbBr_3$-based PeLEDs and to develop efficient stable all-inorganic PeLEDs.

References

[1] Quan L N, Rand B, Richard H F, Mhaisalkar S G, Lee T W and Sargent E H 2019 *Chem. Rev.* **119** 7444

[2] Lozano G 2018 *J. Phys. Chem. Lett.* **9** 3987

[3] Abdi-Jalebi M, Andaji-Garmaroudi Z, Cacovich S, Stavrakas C, Philippe B, Richter J M, Alsari M, Booker E P, Hutter E M, Pearson A J, Lilliu S, Savenije T J, Rensmo H, Divitini G, Ducati C, Friend R H and Stranks D 2018 *Nature* **555** 497

[4] Cao Y, Wang N N, Tian H, Guo J S, Wei Y Q, Chen H, Miao Y F, Zou W, Pan K, He Y R, Cao H, Ke Y, Xu M M, Wang Y, Yang M, Du Kai, Fu Z, Kong D C, Dai D X, Jin Y Z, Li G Q, Li H, Peng Q M, Wang J P and Huang W 2018 *Nature* **562** 249

[5] Lin K B, Xing J, Quan L N, de Arquer F P G, Gong X W, Lu J X, Xie L Q, Zhao W J, Zhang D, Yan C Z, Li W Q, Liu X Y, Lu Y, Kirman J, Sargent E H, Xiong Q H and Wei Z H 2018 *Nature* **562** 245

[6] Zhao X F and Tan Z K 2020 *Nat. Photon.* **14** 215

[7] Tan Z K, Moghaddam R S, Lai M L, Docampo P, Higler R, Deschler F, Price M, Sadhanala A, Pazos L M, Credgington D, Hanusch F, Bein T, Snaith H J and Friend R H 2014 *Nat. Nanotech.* **9** 687

[8] Cho H C, Jeong S H, Park M H, Kim Y H, Wolf Christoph, Lee C L, Heo J H, Sadhanala A, Myoung N S, Yoo S, Im S H, Friend R H and Lee T W 2015 *Science* **350** 1222

[9] Fang Z B, Chen W J, Shi Y L, Zhao J, Chu S L, Zhang J and Xiao Z G 2020 *Adv. Funct. Mater.* **30** 1909754

[10] Xu W D, Hu Q, Bai S, Bao C X, Miao Y F, Yuan Z C, Borzda T, Barker A J, Tyukalova E, Hu Z J, Kawecki M, Wang H Y, Yan Z, Liu X J, Shi Z B, Uvdal K, Fahlman M, Zhang W J, Duchamp M, Liu J M, Petrozza A, Wang J P, Liu L M, Huang W and Gao F 2019 *Nat. Photon.* **13** 418

[11] Zhang L Q, Yang X L, Jiang Q, Wang P Y, Yin Z G, Zhang X W, Tan H, Yang Y M, Wei M Y, Sutherland B R, Sargent E H and You J 2017 *Nat. Commun.* **8** 15640

[12] Wang R, Jia Y L, Zhang Y, Ma X J, Xu Q, Zhu Z X, Deng Y H, Xiong Z H and Gao C H 2020 *Acta Phys. Sin.* **69** 038501 (in Chinese)

[13] Song L, Guo X Y, Hu Y S, Lin J, Fan Y, Zhang N and Liu X Y 2018 *Nanoscale* **10** 18315

[14] Wang Y, Li X M, Sreejith S, Cao F, Wang Z, Stuparu M C, Zeng H and Sun H D 2016 *Adv. Mater.* **28** 10637

[15] Zhang X L, Xu B, Zhang J B, Gao Y, Zheng Y J, Wang K and Sun X W 2016 *Adv. Funct. Mater.* **26** 4595

[16] Zhou G J, Jia X F, Guo S Q, Molokeev M, Zhang J Y and Xia Z G 2019 *J. Phys. Chem. Lett.* **10** 4706

[17] Lee S, Jang C H, Nguyen T L, Kim S H, Lee K M, Chang K, Choi S S, Kwak S K, Woo H Y and Song M H 2019 *Adv. Mater.* **31** 1900067

[18] Song L, Guo X Y, Hu Y S, Lv Y, Lin J, Liu Z Q, Fan Y and Liu X Y 2017 *J. Phys. Chem. Lett.* **8** 4148

[19] Liu X, Guo X Y, Lv Y, Hu Y S, Fan Y, Lin J, Liu X M and Liu X Y 2018 *Adv. Opt. Mater.* **6** 1801245

[20] Lin H, Zhu L, Huang H, Reckmeier C J, Liang C J, Rogach Andrey L and Choy W C H 2016 *Nanoscale* **8** 19846

[21] Wang Y T, He J L, Yang Y C, Zhang Z K and Run L 2019 *ACS Appl. Energ. Mater.* **2** 3419

[22] Cheng L P, Huang J S, Shen Y, , Li G P, Liu X K, Li W, Wang Y H, Li Y Q, Jiang Y, Gao F, Lee C S and Tang J X 2019 *Adv. Opt. Mater.* **7** 1801534

[23] Park M H, Jeong S H, Seo H K, Wolf C, Kim Y H, Kim H, Byun J, Kim J S, Cho H and Lee T W 2017 *Nano Energy* **42** 157

[24] Li N, Song L, Jia Y H, Dong Y F, Xie F Y, Wang L D, Tao S X and Zhao N 2020 *Adv. Mater.* **32** 1907786

[25] Wang M, Tang J, Wang H, Zhang C, Zhao Y S and Yao J N 2020 *Adv. Opt. Mater.* **8** 1901780

[26] Liu Y Y, Xiao H and Goddard W A 2016 *Nano Lett.* **16** 3335